Journal of Power Sources 203 (2012) 288–296

Contents lists available at SciVerse ScienceDirect

Journal of Power Sources

journal homepage: www.elsevier.com/locate/jpowsour

Preparation of structurally modified, conductivity enhanced-p-CuSCN and its application in dye-sensitized solid-state solar cells

E.V.A Premalal[a,*], N. Dematage[a], G.R.R.A. Kumara[a], R.M.G. Rajapakse[a,c], M. Shimomura[b], K. Murakami[b], A. Konno[a,*]

[a] Graduate School of Science and Technology, Shizuoka University, 3-5-1 Johoku, Naka-ku, Hamamatsu, Japan
[b] Research Institute of Electronics, Shizuoka University, 3-5-1 Johoku, Naka-ku, Hamamatsu, Japan
[c] Department of Chemistry, University of Peradeniya, Peradeniya, Sri Lanka

ARTICLE INFO

Article history:
Received 10 September 2011
Received in revised form
14 December 2011
Accepted 15 December 2011
Available online 24 December 2011

Keywords:
CuSCN
Hall measurement
Dye-sensitized solid-state solar cell
AC impedance

ABSTRACT

A method is found to significantly improve the p-type conductivity of CuSCN modified by incorporating triethylamine coordinated Cu(II) sites in its structure. It is done by mixing triethylamine hydrothiocyanate with CuSCN in propyl sulfide solution and allowing it to stand still in the dark for a few weeks in a closed sample tube. XRD and SEM analyses point to the modification of the CuSCN material. The Hall effect measurements clearly show a significant enhancement of hole concentration and hence of p-type conductivity. A maximum conductivity of 1.42 S m^{-1} is achieved for the structurally modified CuSCN compared to that of 0.01 S m^{-1} for ordinary CuSCN. AC impedance analysis of solid-state dye-sensitized solar cells based on this material clearly shows the reduction of bulk resistance of the cell with the use of modified CuSCN. This decrease in resistance has been attributed to the enhancement of conductivity and better pore filing of modified CuSCN inside the TiO_2 matrix. As such, the solar cell performance gradually increases to an optimum value beyond which it decreases. The best result obtained for conversion efficiency is 3.4% at AM 1.5, which is a 41.8% enhancement from the best reported value for a dye-sensitized solid-state solar cell using CuSCN as a hole conducting material. The best efficiency value obtained is 14 times higher than that obtained for the dye-sensitized solid-state solar cell made with ordinary CuSCN.

1. Introduction

The dye-sensitized liquid electrolyte based solar cell (DSC) was first reported by Gratzél et al. in 1991 [1]. Numerous research publications since then show both its theoretical interest and technological importance. A recent report indicates that 11.5% solar conversion efficiency may be achieved [2]. A key challenge for the optimization of device performance is to tackle the problem of inverse correlation between the open circuit voltage, V_{OC}, and the short-circuit current density, J_{SC}, and new strategies employed are expected to solve this problem leading to parameters such as J_{SC} = 22 mA cm^{-2}, V_{OC} = 0.9 V, fill factor FF = 0.75 and hence the efficiency η = 15% as discussed in an excellent review of Kroon et al. [3]. Nevertheless the DSCs suffer from the problems associated with dye desorption, volatility of the solvent and the leachability of the liquid electrolyte due to seal imperfections and the possible reactions of the sealant with the electrolyte, which limit its durability and hence practical applications. The stability tests performed have revealed that the dyes such as N3 and N719 have remarkable stabilities for about 56 million turnovers at 2.5 suns [3]. Hydrophobic dyes such as Z907 and K19 are more suitable at elevated temperatures [3]. Out of large number of electrolyte compositions tested, one with LiI, Lewis bases such as t-butylpyridine and low concentrations of iodine in volatile and less viscous solvents such as acetonitrile, gives highest performance, although life-time testing performed in the dark above 60 °C showed rather limited stability [3]. Among various solutions suggested, the replacement of the liquid electrolyte by a solid polymer electrolyte or a p-type semiconductor is expected to eliminate the problems associated with liquid electrolytes. Much slower diffusion of charge carriers in a solid matrix compared to that in a liquid medium is, however, a major obstacle that might impede the performance of solid state devices. Another serious problem is the unwanted impurities such as water or moisture that would have adverse impact on the chemical stability of the device.

Out of many p-type semiconductors investigated for use as hole conductors, such as $CuAlO_2$ [4,5], NiO [6–13], CuI [14–20], CuSCN [21–28], the latter is of particular interest due to its unique chemical robustness associated with its polymeric structure [29,30]. The solar cell is comprised of highly porous interconnected nanocrystalline TiO_2 particle matrix deposited on a transparent conducting

* Corresponding authors. Tel.: +81 53478 1285; fax: +81 53478 1285.
E-mail addresses: vikum777@gmail.com (E.V.A Premalal), tsakonn@ipc.shizuoka.ac.jp (A. Konno).

0378-7753/$ – see front matter © 2011 Elsevier B.V. All rights reserved.
doi:10.1016/j.jpowsour.2011.12.034

oxide surface in which pores have been filled with p-type CuSCN semiconductor nanoparticles. The TiO_2 particle surfaces are fully covered with anchored light absorbing dye (N719). CuSCN also forms a layer above the TiO_2 surface and is in electronic contact with the platinum particles of the lightly platinum-sputtered conducting tin oxide counter electrode through a graphite particle layer introduced on CuSCN, by rubbing a graphite rod on the CuSCN surface. The working principle of this solar cell has been well documented in the literature [21–28]. In spite of its stability and durability, the major problem associated with this system is its rather poor energy conversion efficiency (η). O'Regan et al. have obtained a η of ~2% at 1 sun with N3 dye and improvements have been suggested by selectively coating recombination "hot spots" of TiO_2 surface sites with a thin outer-layer of Al_2O_3 [27]. The major drawback of CuSCN as p-type semiconductor in this solar cell is its very poor hole conductivity (10^{-4} S cm^{-1}) [21–23,27,28] and consequent slower rate of reduction of oxidized dye molecules thus allowing the recombination of electrons injected to TiO_2 CB with the oxidized dye molecules. In an attempt to increase p-type conductivity of CuSCN, Perera et al. [28] have exposed solid CuSCN to halogen gases such as Cl_2 or to a solution of $(SCN)_2$ in CCl_4 and thereby doped the semiconductor with $(SCN)_2$ to create acceptor levels 2.6 eV below the band gap (3.6 eV) of CuSCN. This modification has enhanced the performance of the solar cell considerably with a 1.64% enhancement of η from 0.75% without SCN doping and 2.39% after SCN doping. This is by far the best recorded efficiency in TiO_2/dye/CuSCN system excluding the preliminary results we published in 2010 [31]. Other such p-type semiconductors tested have their own problems, for instance CuI has the problem of chemical reactivity particularly under oxidizing conditions. It has been revealed that holes generated in TiO_2 with sunlight illumination are sufficient to oxidatively degrade CuI [32]. Semiconductors such as $CuAlO_2$ are not processable and hence introduce technical difficulties in making an efficient solar cell. β-CuSCN, therefore, stands out to be the best material provided that its conductivity can be enhanced sufficiently to enable it to effectively neutralize the oxidized dye molecules. Keeping this in mind, we have investigated means of improving conductivity of CuSCN. We describe here the method we have adopted, characterization of the materials obtained, and the performance of all-solid-state DSSCs fabricated using such conductivity-enhanced β-CuSCN materials.

2. Experimental

2.1. Materials

All chemicals used were purchased from Kanto Chemicals Co. Inc., Tokyo, Japan. Commercial CuSCN is pale brown in color with a little pinkish appearance. Chemically modified CuSCN was prepared by using triethylammonium thiocyanate (THT). The preparation procedures are given below.

2.2. Preparation of THT

Ammonium thiocyanate (4.0 g) was dried under vacuum with stirring in a three-neck round-bottom flask for 30 min ~25% excess triethylamine (12 ml) was then poured into above container and placed in a microwave oven. The mixture was heated at 60 °C for 1 h by microwave with continuous stirring under nitrogen. After the completion of the reaction, as shown in equation 1 (*i.e.*, when the ammonia emission is ceased), the flask was removed from the heater, the content was taken into a separating funnel, 30 ml of hexane was poured in and well shaken. The mixture was then allowed to stand still for two layers to separate. The lower layer that contains THT was then separated (unreacted triethylamine dissolves in hexane layer and was discarded). This procedure was repeated three times for complete removal of triethylamine. The final THT layer obtained was washed with dichloromethane (30 ml) to precipitate out any further unreacted NH_4SCN. THT was then purified by rotary evaporation to remove further remaining hexane and dichloromethane so as to obtain transparent, colorless and viscous liquid [33].

$$(C_2H_5)_3N(l) + NH_4SCN(s) \rightarrow (C_2H_5)_3NHSCN(l) + NH_3(g) \quad (1)$$

2.3. Preparation of modified CuSCN

The structurally modified CuSCN was prepared as follows. CuSCN (0.5 g) was mixed with sufficient amount of THT (0.3 g) to obtain a paste which was then stirred with 10.0 ml of propyl sulfide (PS) and allowed to stand still in the dark in a closed sample tube. The aging of the reaction mixture is shown in color in Fig. 1. The sample shown at one-day reaction time is a clear solution of dissolved species in equilibrium with undissolved CuSCN. As time proceeds, white particles begin to become blackish (plate c), although the solution itself remains colorless for up to 3 days of reaction time. Darkening of the solution phase also begins afterwards (color plates d, e and f) and eventually the whole solution becomes black in color (color plate f) with simultaneous separation of white needle-like crystals. Careful investigation through an optical microscope reveals that the crystals are pink colored polytypes rather than single crystals. A parallel experiment was also done with the same composition of the reaction mixture but purging with N_2 gas to remove any dissolved oxygen in it and allowing to react in the same manner. Interestingly, there was no observable change in the color or appearance of the reaction mixture for even 25 days when it is saturated with N_2 gas though prolong reaction very slowly darkens the solid phase as shown in Fig. 1(g) (possibly due to slow diffusion of air with time). A third experiment done with the same composition of the reaction mixture saturated with O_2 gas, darkened quickly and within 2–3 days both the solid and liquid phases were black in color.

2.4. Characterization of materials

XRD measurements were carried out using the films deposited on the glass plates (or powder for pure CuSCN) from the solution mixture of particular aged reaction period (Rigaku Miniflex X-Ray Diffractometer) and some powders scraped form the deposited films were used for FT-IR measurements where pressed pellets of the mixture, made by sample:KBr in 1:20 mass ratio, were used (JASCO FT-IR-460 plus). SEM Pictures of thin films deposited from the aged solution were taken using a JSM-6320F Scanning Electron Microscope. XPS studies were carried out using thin films deposited on thin FTO plates (Solaronix, Aubonne, Switzerland; 5 mm × 5 mm) from the aged solution mixture at designated time intervals (Shimadzu: ESCA-3400 Electron Spectrometer). Common Data Processing System (COMPRO 10; http://www.sasj.jp/COMPRO/) software was used to find the peak area of the XPS spectrum. The Hall measurements of the films made from 1-day and 20th day reaction mixture were carried out using van der Pauw method (Ecopia Hall effect measurement system HMS-3000). AC impedance analysis of complete solar cell (FTO/TiO_2/N719/CuSCN/Pt-FTO) was measured using a Solartron Sl 1260 Impedance/Gain-Phase Analyzer.

2.5. Fabrication of DSSCs

Mesoporous TiO_2 films were prepared by the procedure described below. Titanium tetra-isopropoxide (8 ml) mixed with propan-2-ol (25 ml) and acetic acid (8.5 ml) was hydrolyzed by

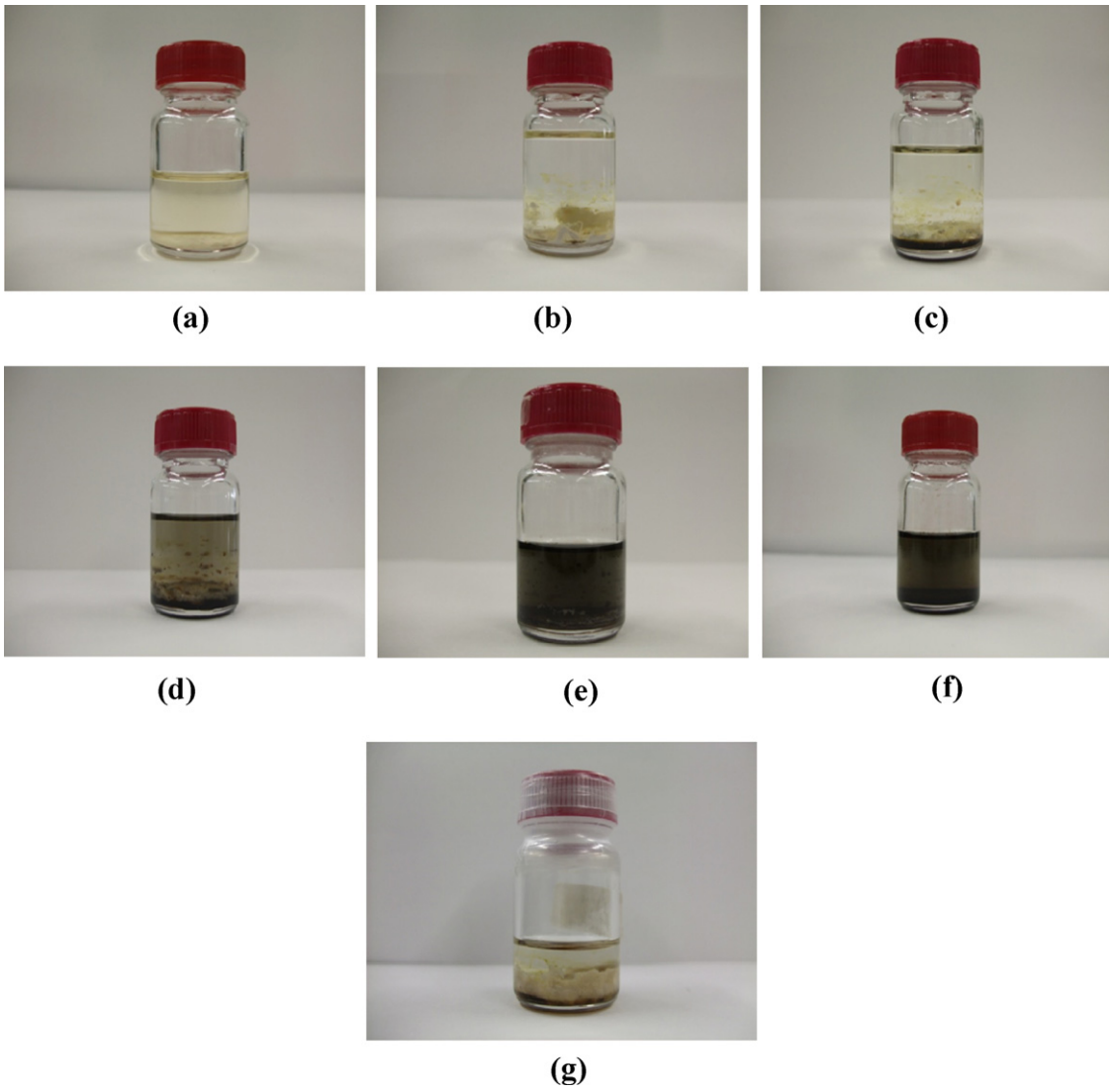

Fig. 1. Color plates of (a) only CuSCN in propyl sulfide, and a reaction mixture containing CuSCN and triethylammonium thiocyanate in propyl sulfide allowed to react for (b) 1 day, (c) 3 days, (d) 5 days, (e) 10 days, and (f) 1 month. The color plate (g) shows a N_2 purged reaction mixture containing CuSCN and triethylammonium thiocyanate in propyl sulfide allowed to react for 25 days. (For interpretation of the references to color in this figure legend, the reader is referred to the web version of this article.)

addition of water (8 ml) to the mixture and agitated mechanically after mixing with 0.7 g of P25 Degussa TiO_2 powder (Nippon Aerosil Co. Ltd., Japan) until the mixture becomes a white viscous colloidal solution. A few drops of this solution was lightly spread on pre-heated (~230 °C) transparent conducting glass sheet (1 cm × 2 cm) (Nippon sheet glass Co. Ltd., Japan; fluorine-doped SnO_2 glass with a sheet resistance 10 Ω) and sintered at 450 °C for 3 min. After allowing the plate to cool, the loose crust on the surface was wiped off and then this process was repeated until a film of ~15 μm was formed. Then N719 (Solaronix, Aubonne, Switzerland); *cis*-diisothiocyanato-bis (2,2′-bipyridyl-4,4′-dicarboxylato) ruthenium(II) bis(tetrabutylammonium) was adsorbed by dipping a TiO_2 film in N719 solution for 15 h at room temperature (4×10^{-4} M, in 1:1 volume ratio of acetonitrile and t-butanol). The CuSCN solution prepared as above at a particular reaction time was spread on a pre-heated (100 °C) dye-coated TiO_2 film by dropwise addition, allowing time to evaporate the solvent. The thickness of the CuSCN film was ~3 μm from the top of the TiO_2 surface. Then IV measurements were carried out by applying a thin layer of graphite film on top the CuSCN films and having platinum sputtered FTO glass plate as a counter electrode (AM 1.5, 100 mW cm^{-2}, JASCO, CEP-25BX).

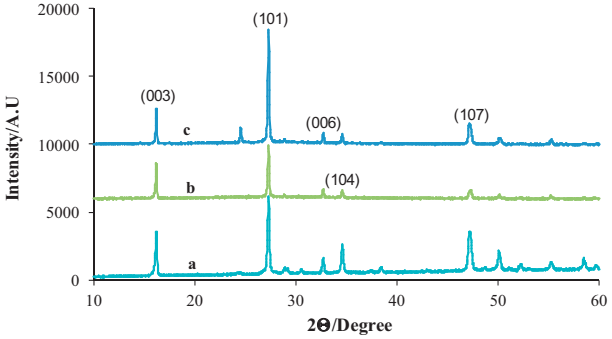

Fig. 2. The XRD spectra of CuSCN film prepared by the reaction mixture containing CuSCN and triethylammonium thiocyanate in propyl sulfide allowed to react for (b) 1 day, (c) 20 days, and (a) pure CuSCN.

3. Results and discussions

3.1. Characterization of CuSCN products

Fig. 2 shows the XRD spectra of CuSCN film prepared by the reaction mixture containing CuSCN and triethylammonium thiocyanate

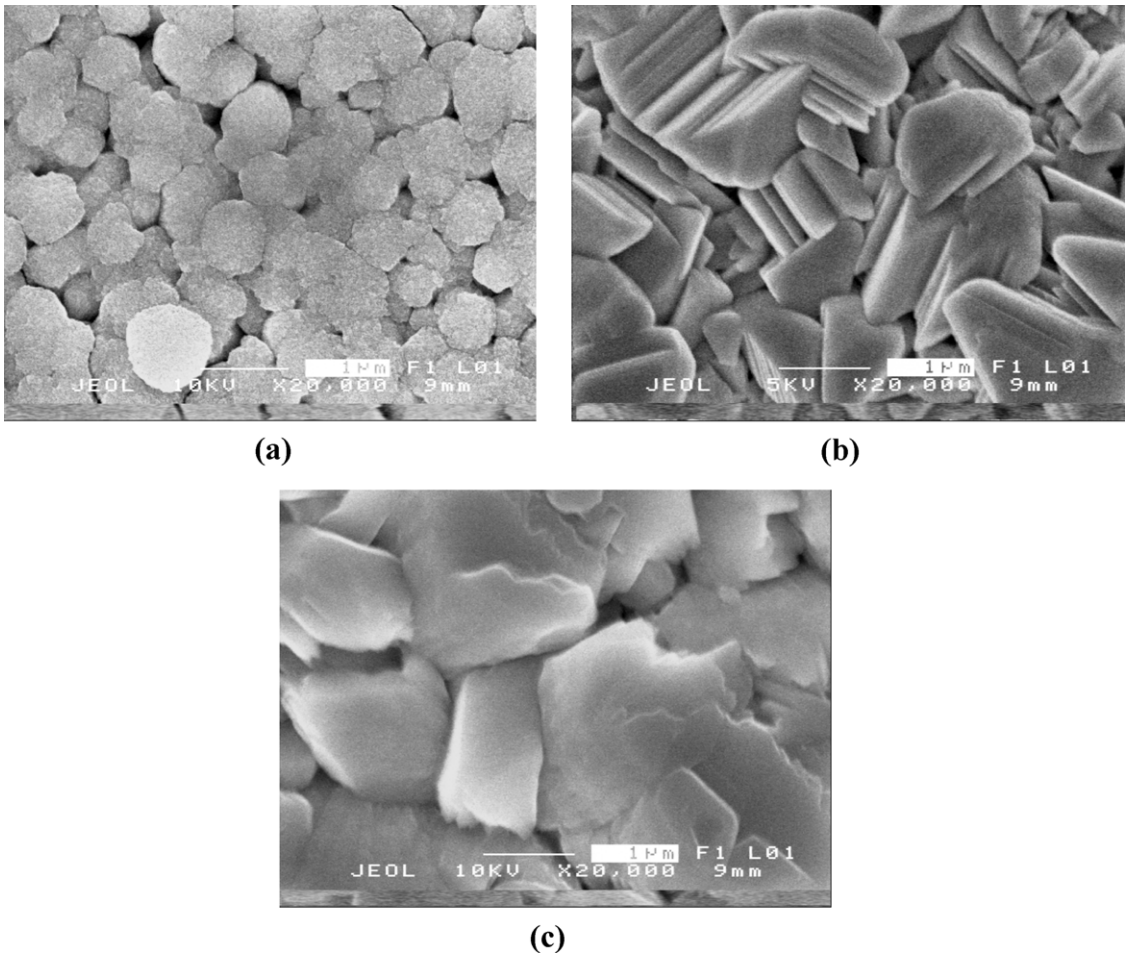

Fig. 3. The SEM images of (a) CuSCN, (b) CuSCN treated with triethyammonium hydrothiocyanate in propyl sulfide for 1 days, and (c) CuSCN treated with triethyammonium hydrothiocyanate in propyl sulfide for 20 days on FTO substrate.

in propyl sulfide at different reaction times and that of pure CuSCN. All the peaks of spectra 'b' corresponding to the CuSCN obtained from one day reaction mixture, consist of only CuSCN characteristic peaks as shown in Fig. 2 (JSPDS 29-0581). However, in spectra c, from a 20th day reaction mixture, an additional peak is appeared at $2\theta = 24.6$. This appearance of new peak suggests that the crystal structure of CuSCN has slightly changed after allowing CuSCN to react with triethylammonium thiocyanate in the propyl sulfide medium.

Further evidence for the change of structure is highlighted in the Scanning Electron Micrographs of the compounds which are shown in Fig. 3. The texture of CuSCN consists of plate-like discs of nearly 100 nm in diameter as can be seen in Fig. 3(a). The discs have a layered structure. When treated with THT, the crystalline structure of such modified CuSCN is completely different to that of pure CuSCN. The former consists of regular prismatic morphology with significantly enhanced crystal size (Fig. 3(b) and (c)). The crystallinity and the crystallite size has increased as the material reacts with triethylammonium thiocyanate in the propyl sulfide medium.

The XPS studies of the samples also provide independent evidence as to the composition of the reaction products when CuSCN is allowed to react with THT in PS. The atomic percentages were calculated using the percentage of corrected area of the corresponding elements and are given in Table 1. The XPS spectra of the unmodified CuSCN samples purchased commercially has Cu:S:N atomic ratio of 1:1:1 suggesting that to be pure cuprous thiocyanate or at least the impurity levels are too small to be detected by XPS. Based on the data given in Table 1, the Cu:S:N atomic ratios of ~1:1:1, 10:14:17, 10:16:17, 10:34:41 could be deduced for the samples prepared from the solution phase that had reacted for 5, 20, 30 and 40 days. A parallel experiment done with an N_2-purged sample does not show any visible color change up to about 25 days. However, a slight darkening of the reaction mixture is observed at the end of 25th day of reaction, when a sample deposited from the solution phase has the Cu:S:N composition 10:11:10 as determined by XPS studies.

Table 1
Atomic percentages calculated from XPS spectrum for the solid samples deposited from the solution phase of the reaction mixture of CuSCN and triethylammoniumthiocyanate in propyl sulfide at different reaction intervals, and the sample deposited after 25 days reaction time from a nitrogen purged reaction mixture.

Reaction time/days	5	20	30	40	25 (N_2 purged)
N 1S	17.2	18.0	16.9	17.4	13.9
S 2P	18.2	14.2	15.7	14.4	15.4
Cu 2p3/2	18.2	10.4	9.7	4.2	13.1

Interestingly, the composition of the propyl sulfide soluble component in the reaction mixture varies with reaction time when allowed to react for a long period of time. Up to about 5 days, the composition hardly changes so that Cu:S:N ratio remains at 1:1:1. The color plates (Fig. 1(b) and (c)) also show that there is hardly any change in the color or appearance of the solution phase up to 5 days. However, a darkening of the solution phase of the reaction mixture begins at the 10th day of reaction time. There are two important facts worth noticing from 10th day to 30th day of reaction time *viz.* (i) the atomic compositions of the samples obtained

are in the order of Cu < S < N and (ii) the amounts of N and S gradually increase with reaction time. These data are reproducible, and indicate that some of the copper ions must be present as Cu(II) in these samples, giving a SCN:Cu ratio greater than one. This is possibly due to oxidation of some Cu(I) sites by $(SCN)_2$ gas produced and trapped within the solid samples (*vide infra*) which is also in agreement with the XRD data given in Fig. 2, which demonstrate structural changes taking place in the system. The fact that atomic percentage of N is greater than that of S suggests that some species containing N but not containing S must be present in the material.

The FT-IR data shown in Fig. 4 give clear evidence to the presence of triethylamine in the solid samples deposited from the solution phase of the reaction mixture. When CuSCN is allowed to react with THT in PS, the CH stretching band can be clearly seen at ~2980 cm^{-1} [see Fig. 4(i)]. Note that this band is broad and intense in THT [marked b in Fig. 4(i)] and is obviously absent in CuSCN. However, as CuSCN reacts with THT, this band begins to appear and is significant in the sample drawn from 30th day of aging [marked d in Fig. 4(i)]. The C≡N stretching band of SCN^- ion falls in the range of 2050–2200 cm^{-1} and is clearly visible in the spectrum of THT where free SCN^- ions present give rise to this absorption. In the case of CuSCN, the SCN^- ions occupy in the lattice positions and are coordinated to Cu *via* S and N. The C≡N band of CuSCN is, therefore, shifted to 2180 cm^{-1}. Interestingly the samples drawn from the 30th day reaction mixture of CuSCN and THT in PS have bands corresponding to C≡N centered at 2050 cm^{-1} and 2180 cm^{-1} [see Fig. 4(ii)]; the latter is likely to be due to the C≡N stretching vibration of trapped $(SCN)_2$ and SCN^- in the interstitial positions of the lattice, while the former is obviously due to vibrations of C≡N in lattice SCN^- ions as in CuSCN. The evidence to support the ruling out of the possibility of having THT trapped within CuSCN lattice comes from the N—H vibration in THT which appears around 3450 cm^{-1} in THT which is totally absent when CuSCN is allowed to react with THT (Fig. 4(iii)). The presence of C—H, C—C and C≡N vibrations in both THT and CuSCN treated with THT and the absence of N-H in the CuSCN samples treated with THT suggest that only triethylammine is inserted in the lattice after removing H^+ from THT. The bands in the range of 1000–1200 cm^{-1} may be assigned for the stretching modes of C—N and C—C bonds and the rocking mode of the methyl group of triethylamine (Fig. 4(iv)).

Fig. 5 shows the AC-impedance spectra of the solar cell FTO/TiO_2/N719/CuSCN/Pt-FTO prepared from the reaction mixture containing CuSCN and triethylammonium thiocyanate in propyl sulfide, and aged for 30 days. It was recorded over the frequency range of 0.05–10^7 Hz, under dark conditions and at different forward bias voltages. The characteristic arcs of this solid state solar cell are slightly different from those of other reported solid state cells such as CuSCN on ZnO and Spiro-OMeTAD on TiO_2 [34,35]. To understand the characteristic behavior of each arc, the equivalent circuits shown in Fig. 6 are proposed [34–37]. At zero bias potential, the impedance diagram consists of three consecutive arcs; a very small arc in the high frequency region, a large arc at moderate frequency and another arc at low frequency. Under dark conditions and with zero bias voltage, TiO_2 has a very high resistivity (>10^{10} Ω cm) [38] and hence transmission lines in TiO_2 and TiO_2/CuSCN interface components are excluded from the equivalent circuit and then it simplifies to that shown in Fig. 6(b). Therefore, the arcs at zero bias potential can be assigned as follows, *i.e.*, a small arc in very high frequency region which is likely to be corresponding to the CuSCN/Counter electrode interface, an arc at moderate frequencies which might correspond to the hole transportation in CuSCN (the Warburg impedance pattern of hole diffusion can be seen in the high frequency region, as shown in the inset of Fig. 5), with an arc at low frequencies which might correspond to the FTO/CuSCN interface. Z_d is the Warburg element corresponding to the mass diffusion of ions such as SCN^- in the

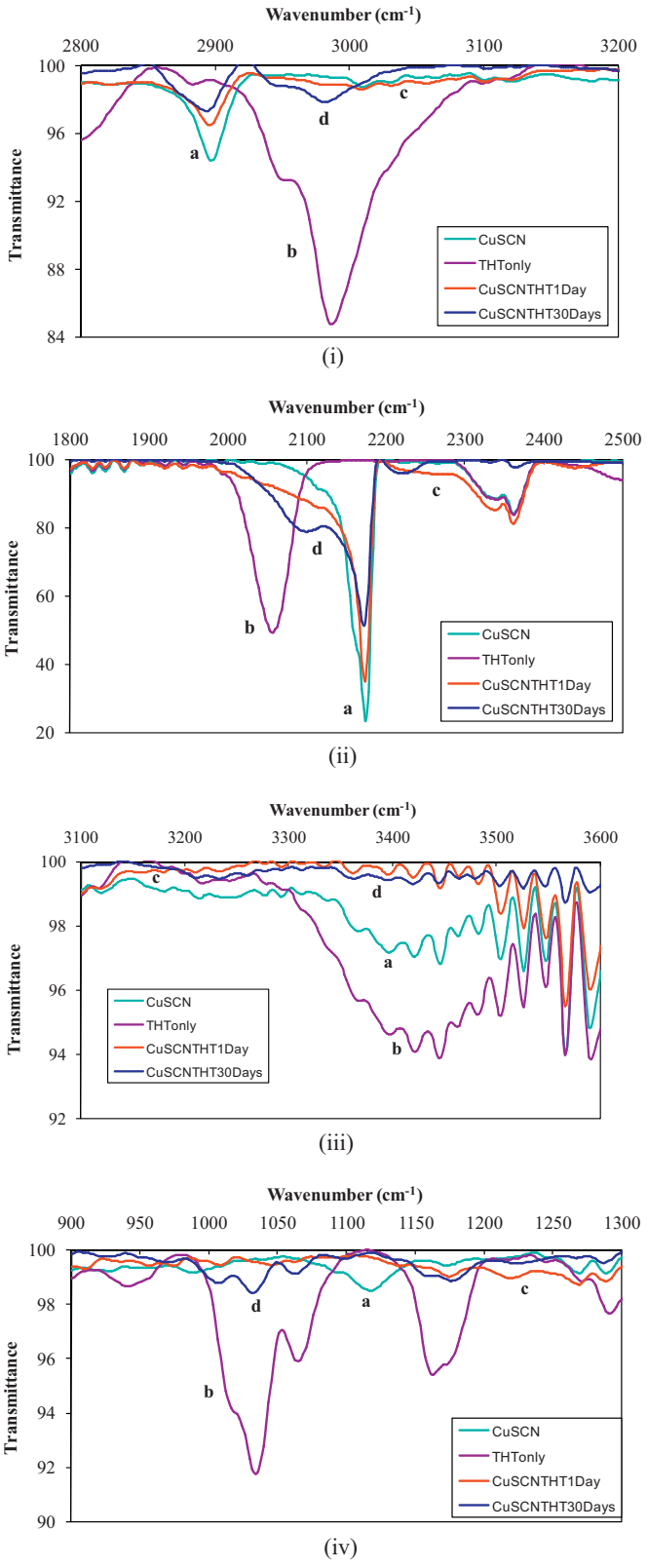

Fig. 4. The FT-IR spectra of CuSCN, Triethylammoniumhydrotiocyanate, and CuSCN and triethylammoniumhydrothiocyanate allowed to react in propyl sulfide for 1 day and 30 days. Useful regions are enlarged for clarity.

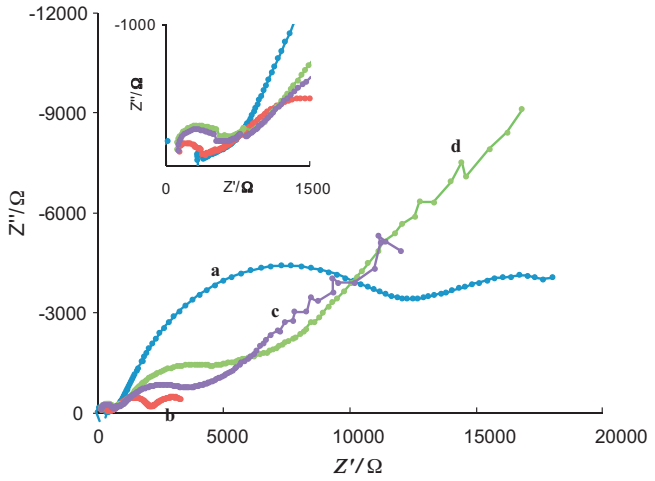

Fig. 5. Nyquist plots of impedance measurements of the solar cell (FTO/TiO_2/N719/CuSCN/Pt-FTO) where CuSCN has been deposited from 30th day of reaction mixture of CuSCN and triethyl ammonium thiocyanate in propyl sulfide, recorded at different applied forward bias voltages under dark conditions. The bias voltages are (a) 0.0 V (b), 0.2 V, (c) 0.5 V, and (d) 0.6 V. The inset shows the same impedance spectra in the high frequency regions.

modified CuSCN material and this impedance is negligible at zero bias voltage due to very small current flowing through the cell as shown in Fig. 5. At 0.2 V forward bias voltage, where still $r_t \gg R_{t_{CuSCN}}$, arcs similar to those observed at zero bias voltage appear but with decreased diameters (and hence corresponding resistance). In this case also Z_d is still negligible. Therefore the equivalent circuit of the solar cell is simplified to the components shown in Fig. 6(b). When the forward bias voltage is increased to 0.5 V or 0.6 V, the Fermi level in TiO_2 approaches the lower edge of the conduction band and the electron transport resistance in TiO_2 (r_t) becomes smaller due to increased electron density. In this case the equivalent circuit of Fig. 6(a) simplifies to the one shown in Fig. 6(c). It consists of very small arc in the very high frequency region corresponding to the CuSCN/Counter electrode interface, a medium arc at moderate frequency corresponding to the TiO_2/CuSCN interface and the Warburg pattern in the low frequency region corresponding to the mass diffusion of ions such as SCN^- ions in the modified CuSCN as shown in Fig. 5(c) and (d). At these potentials, the Warburg component of hole diffusion is also visible in the high frequency region of Nyquist plot as shown in the inset of Fig. 5. When $r_t \ll R_{t_{CuSCN}}$, at higher potential (*i.e.*, the TiO_2 is highly conducting), the FTO/CuSCN charge transfer resistance should be much larger than that at lower forward bias potentials ($\sim\leq$0.2 V) where TiO_2 become insulating. The charge transfer resistance (recombination resistance) of TiO_2/CuSCN interface at 0.6 V forward bias potential is higher than that at 0.5 V forward bias voltage. This means that the recombination resistance at the TiO_2/CuSCN interface is very large under DSC operating conditions of the solar cell. Here we first time reveal the behavior of characteristic arcs of impedance spectra of solid state solar cell (TiO_2/Dye/modified CuSCN) based on previous reported models [34–37]. Therefore these interpretations are tentative and further research is needed to completely understand the impedance spectra of this cell.

Mora-Sero et al. have performed AC impedance analysis for a ZnO nanowire/CdSe/CuSCN solar cell and obtained a simple pattern for the impedance spectra [34]. Due to the presence of high intrinsic n-doping and its single-crystal character, ZnO is a material with good electron transport characteristics even in the dark at zero bias voltage. Therefore they have assumed that ZnO becomes short circuited. To the best of our knowledge, this is the only paper which has discussed the AC impedance analysis in detail in a solar cell based on CuSCN as a hole conducting material. Here the authors used pure CuSCN which has a high resistivity. Therefore, their ZnO/CdSe/CuSCN solar cell system shows a simple equivalent circuit arrangement consisting of only parallel connection of charge transfer resistance and chemical capacitance at the ZnO/CuSCN interface regardless of the bias voltages. However, our modified CuSCN material has much low resistivity due to the presence of doped SCN^- ions and triethylamine coordinated Cu(II) sites in the lattice so that the equivalent circuit of the solar cell becomes more complex.

Table 2
Parameters of the equivalent circuit in Fig. 6(b) for solid-state DSSCs prepared from (b) 1 day, (c) 30 days of reacting CuSCN with triethyl ammonium thiocyanate in propyl sulfide.

Cell	$R_{t_{CuSCN}}$ (MΩ)	$R_{C_{FTO}}$ (MΩ)
b	25.70	51.49
c	13.87	16.13

Fabregat-Santigo et al. have performed AC impedance analysis for the TiO_2/Dye/Spiro-OMeTAD system but under illumination and at over 0.4 V forward bias voltages [35]. They observed a small arc in the high frequency region for TCO/underlayer/OMeTAD interface and a large arc at low frequencies for the TiO_2/OMeTAD interface. Their analysis is reasonable for a highly resistive OMETAD at higher forward bias potentials.

Fig. 7 shows the AC-impedance spectra of complete solar cell (FTO/TiO_2/N719/CuSCN/Pt-FTO) prepared from the reaction mixture containing CuSCN and triethylammonium thiocyanate in propyl sulfide allowed to react for different time periods which were recorded over a frequency range of 0.05–10^7 Hz, in the under dark and at zero bias voltage, where TiO_2/CuSCN interface properties are not observed in the Nyquist plots as explained above (see Fig. 6(b)). The impedance plot of the cell prepared from pure CuSCN (Fig. 5(a)) shows only a vertical pure capacitive line but with increased days of reaction time, the Nyquist plots (Fig. 5(b) and (c)) show three consecutive arcs as explained above. Pure CuSCN has very high resistivity, and therefore Nyquist plot for the cell prepared from pure CuSCN shows a pure capacitive line. The circuit parameters were calculated by curve fitting with Z-view software and the corresponding resistance values are given in Table 2 and ω_{max} values are marked in Fig. 7. The diameter of each arc in cell b prepared from a one day reaction mixture of solution are larger than those of cell c, prepared using a 30 day reaction mixture. That is, the charge transfer resistance at the interface of FTO/CuSCN ($R_{C_{FTO}}$), and hole transport resistance in the CuSCN material ($R_{t_{CuSCN}}$), have been considerably reduced in cell c compared to those for cell b as is clearly seen in Table 2. This reduction clearly indicates the conductivity enhancement of the CuSCN material prepared from aged reaction mixtures. The ω_{max} increment in cell c is attributed to the fast transport and transfer of charges in CuSCN material with enhanced conductivity.

The important parameters to consider in the modified CuSCN are the p-type conductivity, hole density and hole mobility. We have, therefore, carried out the Hall Effect measurements of CuSCN samples prepared from 1-day and 20th-day reaction mixtures using the van der Pauw method. Hall measurements which give rise to positive Hall coefficient reveal the p-type nature of the CuSCN material. The conductivity values obtained from the Hall measurements of the samples made from 1st day and 20th day reaction mixture are 0.31 S m^{-1} and 1.42 S m^{-1}, respectively. These values are in very good agreement with AC impedance measurements and provide yet another independent proof for the conductivity enhancement of the samples prepared from the aged reaction mixtures. The Hall Effect measurements also provide the hole concentrations of the films. The

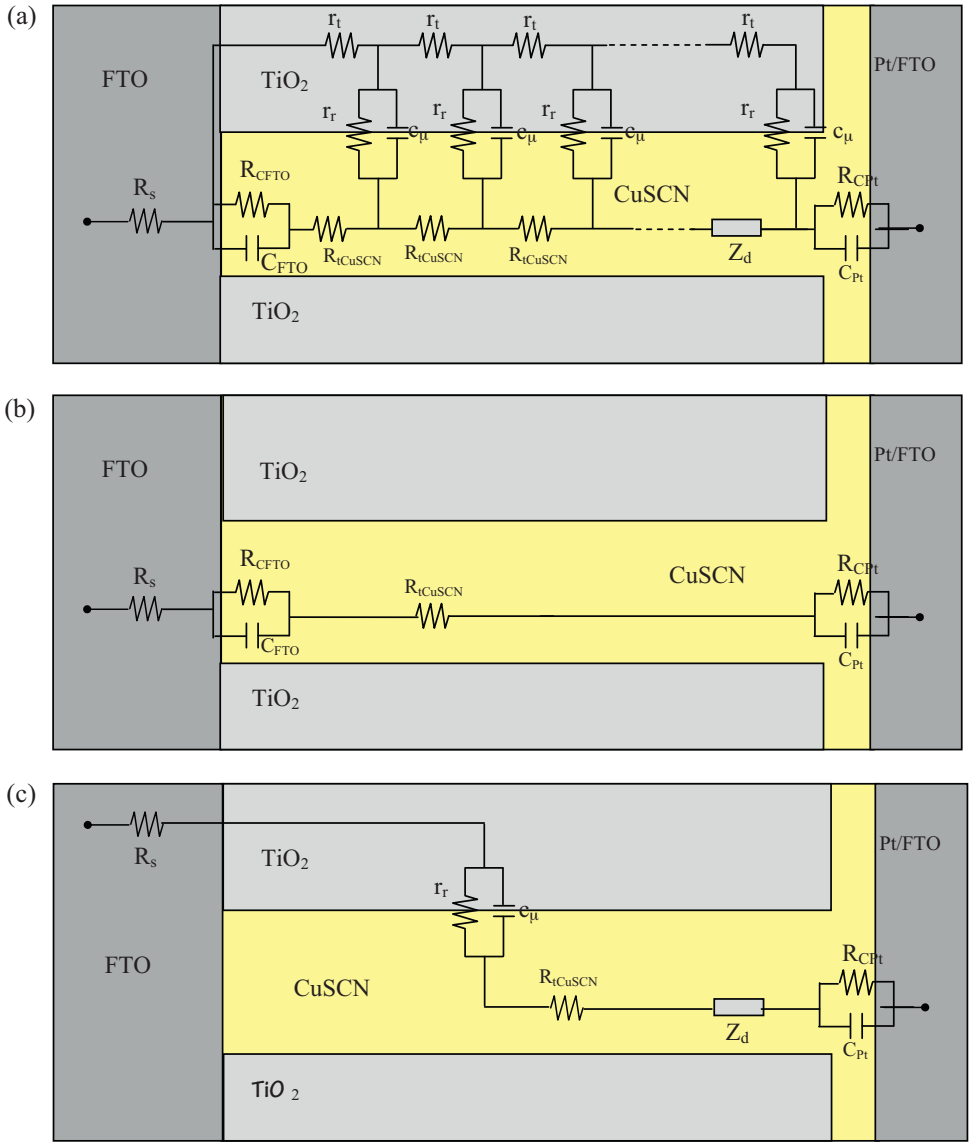

Fig. 6. (a) The equivalent circuit for the complete solar cell FTO/TiO_2/Dye/CuSCN/Pt-FTO. (b) Simplified circuit when TiO_2 is insulating at zero bias voltage. (c) Simplified equivalent circuit where TiO_2 is in a conductive state (at 0.5 V and 0.6 V forward bias potentials). r_t is the electron transport resistance in TiO_2, $R_{C_{FTO}}$ is the charge transfer resistance at FTO/CuSCN interface, C_{FTO} is the constant phase element (CPE) at the point of triple contact of FTO/CuSCN/TiO_2, r_r is the charge transfer resistance (recombination resistance) at the TiO_2/CuSCN interface, C_μ is the CPE at TiO_2/CuSCN interface, $R_{t_{CuSCN}}$ is the hole transport resistance at CuSCN, Z_d is the Warburg impedance for ion diffusion, $R_{C_{Pt}}$ is the charge transfer resistance at the CuSCN/Pt-FTO interface, and C_{Pt} is the CPE at the CuSCN/Pt-FTO interface.

hole concentrations calculated for CuSCN samples prepared from 1st day and 20th day reaction period are $7.04 \times 10^{15}\,cm^{-3}$ and $8.22 \times 10^{16}\,cm^{-3}$, respectively. The high hole concentration (~11 times) of the sample at 20th-day reaction period attributes to the increment of SCN^- trapping in the film made from aged reaction mixture.

Hole conductivity of the sample is the product of charge, hole concentration and the mobility of holes. Therefore, the mobility of the holes of the samples made from 1st day and 20th day reaction mixture can be calculated to be $2.73\,cm^2\,V^{-1}\,s^{-1}$ and $1.08\,cm^2\,V^{-1}\,s^{-1}$ respectively. Interestingly, the hole mobility of the best-conducting sample has been reduced by a factor of 2.5 from that of the unmodified sample. This is a striking result where a significant increase in hall density and decrease in hole mobility with reaction time cause holes capable of recombining with injected electrons in the CB of TiO_2. Therefore, obviously the solar cell performance goes through a maximum and beyond which it decreases.

We therefore propose the following reaction scheme which is likely to be responsible for the reactions leading to the formation of p-type conductivity enhanced CuSCN materials in the reaction mixture. Interestingly, if CuSCN is dissolved in PS and triethylamine is added (instead of THT) there is no immediate color change but a few hours later the solution becomes light green in color and after two days later color becomes light green to brown in color. This is most likely due to the coordination complex formed by the coordination of triethylamine and SCN^- ions to Cu(I) ions. The black compounds formed in the reaction mixture of CuSCN and THT in PS are due to forming Cu(II) complexes formed by the following reactions.

$$[(C_2H_5)_3NH]^+ \leftrightarrow (C_2H_5)_3N + H^+ \quad (2)$$

$$4Cu(I) + O_2 + 4H^+ \rightarrow 4Cu(II) + 2H_2O \quad (3)$$

$$2(C_2H_5)_3N + Cu(II) + 2SCN^- \rightarrow [(C_2H_5)_3N]_2Cu(SCN)_2 \quad (4)$$

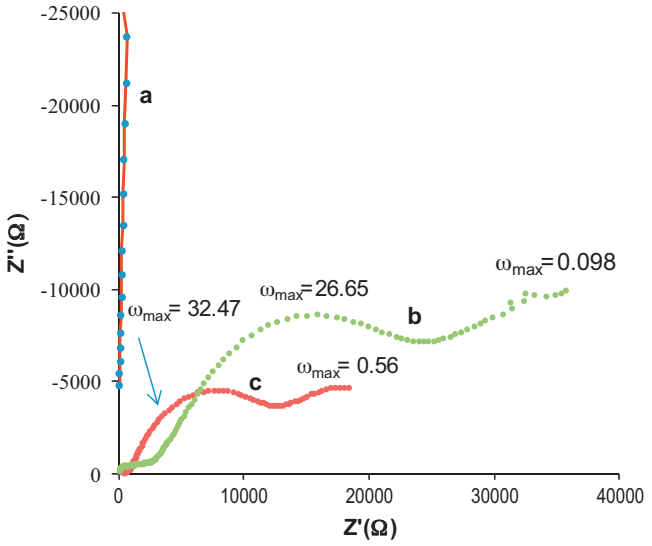

Fig. 7. Nyquist plots for the impedance measurements of the solar cell (FTO/TiO_2/N719/CuSCN/Pt-FTO) prepared from (a) pure CuSCN, (b) 1 day, and (c) 30 days of reacting CuSCN with triethyl ammonium thiocyanate in propyl sulfide.

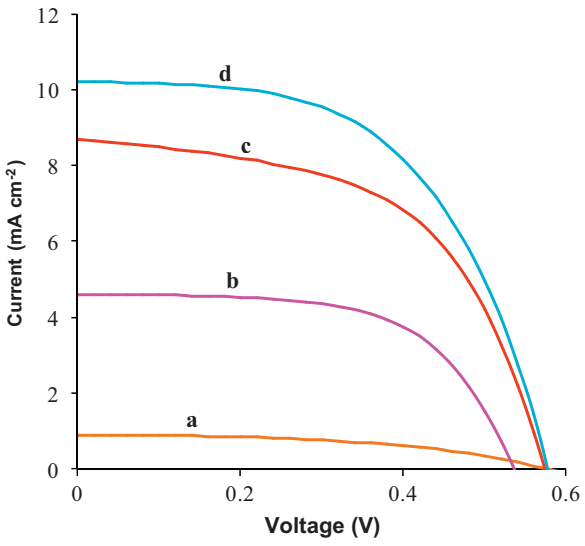

Fig. 8. The I–V curves of the FTO/TiO_2/N719/CuSCN/Pt-FTO cells prepared using (a) pure CuSCN, (b) 1 day, (c) 10 days, and (d) 20 days of reacting CuSCN with triethyl ammonium thiocyanate in propyl sulfide.

Note also that the formation of species such as $\{[(C_2H_5)_3N]_3Cu(SCN)\}^+$ and $\{[(C_2H_5)_3N]Cu(SCN)_3\}^-$ is very likely.

If triethylamine is used instead of triethylammonium ion then there is no source for H^+ ions and the reaction 3 is thus not possible. This explains why black compounds are not formed when triethylamine is used instead of triethyl ammonium ions.

The cupric thiocyanate can spontaneously decompose to give cuprous thiocyanate and thiocyanogen gas:

$$2Cu(SCN)_2 \rightarrow 2CuSCN + (SCN)_2 \quad (5)$$

Some of the sites in the material can have triethylamine coordinated Cu(II) and hence $[(C_2H_5)_3N]_2Cu(SCN)_2$ could decompose giving $[(C_2H_5)_3N]_2CuSCN$ and $(SCN)_2$ according to the following reaction.

$$2[(C_2H_5)_3N]_2Cu(SCN)_2 \rightarrow 2[(C_2H_5)_3N]_2CuSCN + (SCN)_2 \quad (6)$$

The $(SCN)_2$ trapped within the interstitial positions can oxidize some Cu(I) sites to Cu(II) according to the reaction

$$(SCN)_2 + 2Cu(I) \rightarrow 2SCN^- + 2Cu(II) \quad (7)$$

Note that the redox reactions (3) and (7) are thermodynamically allowed according to the standard electrode potentials of Cu(II)/Cu(I), O_2/H_2O and $(SCN)_2/SCN^-$ redox couples [+0.16 V, +1.23 V and +0.43 V respectively at 25 °C]. We explain the increase in p-type conductivity with time is due to formation of increased amounts of hole bearing Cu(II) sites in the CuSCN lattice. The presence of some triethylamine is justified by the XPS results which show higher N content compared to S content in the compounds.

The formation of pink colored double-salt type $Cu_2[(CH_3)_3NH^+](SCN)_3$ from the solution of Cu(I), SCN^- and trimethylammonium ions in acetone has already been documented [39]. However, in our reaction system the structural modification of CuSCN through the coordination of triethylamine followed by redox reactions given in the above scheme are more likely than forming such a double salt compound. Also the formation of polythiocyanagen $(SCN)_x$ in this reaction mixture has been revealed [21,22] which supports the reaction scheme proposed above. We, therefore, believe that this is a very successful method for the preparation of p-type CuSCN with significantly enhanced hole conductivity.

Table 3
I–V parameters for FTO/TiO2/N719/CuSCN/Pt-FTO DSSCs prepared using CuSCN taken from the solution phase of the reaction mixture of CuSCN and triethylammonium thiocyanate in propyl sulfide at different reaction times.

Reaction time/days	J_{SC} (mA cm^{-2})	V_{oc} (V)	FF	η%
0 (No THT)	0.90	0.576	0.477	0.25
1	4.59	0.535	0.609	1.50
3	5.11	0.549	0.580	1.63
5	7.83	0.569	0.554	2.47
10	8.67	0.573	0.548	2.73
15	10.22	0.576	0.553	3.26
20	10.52	0.578	0.556	3.39
30	10.00	0.561	0.522	2.93

3.2. Solar cell characteristics

We have used such conductivity enhanced CuSCN in fabricating solid-state dye-sensitized solar cells as described below. The TiO_2/N719 Dye/CuSCN solar cells were fabricated using the usual procedure described in Section 2 using CuSCN from the reaction solution at different reaction times. The IV characteristics of some DSSCs are given in Fig. 8 and the IV parameters of all cells measured are extracted in Table 3.

As the reaction time is increased, the p-type conductivity of CuSCN enhances and consequently the open circuit voltage (V_{OC}), short-circuit current density (J_{SC}) and the overall conversion efficiency (η) show progressively increase up to 20 days of reaction time. The fill factor (FF) also increases initially and then slightly decreases eventually reaching a plateau at around 0.55 up to 20 days of reaction time (Table 3). This is also in agreement with the progressive increase of the amount of holes in CuSCN as the reaction proceeds. Although the p-type conductivity of CuSCN progressively increases even up to 30 days of reaction time, the solar cell performance of the DSSC made using CuSCN with 30 days reaction time is inferior to that made using CuSCN with 20 days reaction time. The enhancement of conductivity causes the decrease in FF. But efficient regeneration of dye thus efficient charge injection to TiO_2 will increase the Fermi level of TiO_2 slightly in turn improving V_{OC}.

The best result is obtained when CuSCN at the 20 days of reaction period is employed which is 3.39% at AM 1.5 simulated sun light as compared to the best reported 2.39% under the same conditions showing a 41.8% enhancement of the efficiency[28]. According to

our results, the solar cell fabricated with pure CuSCN gives an efficiency of 0.25% and that with 20 days of reaction time 3.39% thus indicating ~14 times enhancement of efficiency. The improvements shown are promising and open up a way to tailor-make CuSCN to possess right conductivity to efficiently compete with the oxidized dye molecules against recombination. Together with extra-ordinary stability of the polymeric form of CuSCN, fabrication of durable and stable all-solid-state DSSCs with considerable efficiency could be realized.

4. Conclusions

Conductivity enhanced, structurally modified CuSCN was prepared by mixing triethylamine hydrothiocyanate with CuSCN in propyl sulfide solution and allowing to stand still in the dark for different periods of time in a closed sample tube. Enhancement of conductivity was observed in Hall effect measurements while the modification of structure of CuSCN was observed by XRD analysis. AC impedance analysis further indicates the conductivity enhancement of the modified CuSCN materials. The use of such conductivity-enhanced CuSCN in all-solid-state dye-sensitized solar cells (DSSCs) gives improved performance measured by I–V characteristics. The best result obtained for the energy conversion efficiency is 3.39% at AM 1.5 and is 14 times higher than that obtained for the DSSC made with ordinary CuSCN.

References

[1] B. O'Reagan, M. Gràtzel, Nature 353 (1991) 737.
[2] C.Y. Chen, M. Wang, J.Y. Li, N. Pootrakulchote, L. Alibabaei, C.H. Ngoc-le, J.D. Decoppet, J.H. Tsai, C. Gratzel, C.G. Wu, S.M. Zakeeruddin, M. Gratzel, ACSNANO 3 (2009) 3103.
[3] J.M. Kroon, N.J. Bakker, H.J.P. Smit, P. Liska, K.R. Thampi, P. Wang, S.M. Zakeeruddin, M. Gra¨tzel, A. Hinsch, S. Hore, U. Wu¨rfel, R. Sastrawan, J.R. Durrant, E. Palomares, H. Pettersson, T. Gruszecki, J. Walter, K. Skupien, G.E. Tulloch, Prog. Photovolt. Res. Appl. 15 (2007) 1.
[4] H. Kawazoe, M. Yasukawa, H. Hyodo, M. Kurita, H. Yanagi, H. Hosono, Nature 389 (1997) 939.
[5] J.J. He, H. Lindström, A. Hagfeldt, S.E. Lindquist, J. Phys. Chem. B 103 (1999) 8940.
[6] C. Lévy-Clément, Nanostructured Materials for Solar Energy Conversion, 2006, p. 447.
[7] L. Li, E.A. Gibson, P. Qin, G. Boschloo, M. Gorlov, A. Hagfeldt, L. Sun, Adv. Mater. (2010), doi:10.10002/adma.200903151.
[8] J. Bandara, H. Weerasinghe, Sol. Energy Mater. Sol. Cells 85 (2005) 385.
[9] S.S. Kim, K.W. Park, J.H. Yum, Y.E. Sung, Sol. Energy Mater. Sol. Cells 90 (2006) 283.
[10] Y.M. Lee, C.H. Lai, Solid State Electron. 53 (2009) 1116.
[11] Y.M. Lee, C.H. Hsu, H.W. Chen, Appl. Surf. Sci. 255 (2009) 4658.
[12] K.H. Wong, K. Ananthanarayanan, S.R. Gajjela, P. Balaya, Mater. Chem. Phys. 125 (2011) 553.
[13] L. Cattin, B.A. Reguig, A. Khelil, M. Morsli, K. Benchouk, J.C. Bernède, Appl. Surf. Sci. 254 (2008) 5814.
[14] K. Tennakone, V.P.S. Perera, I.R.M. Kottegoda, G.R.R.A. Kumara, J. Phys. D: Appl. Phys. 32 (1999) 374.
[15] W.C. Sinke, M.M. Wienk, Nature 395 (1998) 544.
[16] B. Li, L.D. Wang, B. Kang, P. Wang, Y. Qiu, Sol. Energy Mater. Sol. Cells 90 (2006) 549.
[17] K. Tennakone, G.R.R.A. Kumara, A.R. Kumarasinghe, K.G.U. Wijayantha, P.M. Sirimanne, Semicond. Sci. Technol. 10 (1995) 1689.
[18] L.Yang, Z. Zhang, S. Fang, X. Gao, M. Obata, Solar Energy 81 (2007) 717.
[19] Q.B. Meng, K. Takahashi, X.T. Zhang, I. Sutanto, T.N. Rao, O. Sato, A. Fujishima, Langmuir 19 (2003) 3572.
[20] A. Konno, T. Kitagawa, H. Kida, G.R.A. Kumara, K. Tennakone, Curr. Appl. Phys. 5 (2005) 149.
[21] K. Tennakone, A.R. Kumarasinghe, P.M. Sirmanne, G.R.R.A. Kumara, Thin Solid Films 261 (1995) 307.
[22] G.R.R.A. Kumara, A. Konno, G.K.R. Senadeera, P.V.V. Jayaweera, D.B.R.A. De Silva, K. Tennakone, Sol. Energy Mater. Sol. Cells 69 (2001) 195.
[23] B. O'Regan, D.T. Schwartz, Chem. Mater. 10 (1998) 1501.
[24] B. O'Regan, D.T. Schwartz, S.M. Zakeeruddin, M. Gratzel, Adv. Mater. 12 (2000) 1263.
[25] B. O'Regan, D.T. Schwartz, Chem. Mater. 7 (1995) 1349.
[26] B. O'Regan, F. Lenzmann, R. Muis, J. Wienke, Chem. Mater. 14 (2002) 5023.
[27] B. O'Regan, S. Scully, A.C. Mayer, J. Phys. Chem. B 109 (2005) 4616.
[28] V.P.S. Perera, M.K.I. Senevirathna, P.K.D.D.P. Pitigala, K. Tennakone, Sol. Energy Mater. Sol. Cells 86 (2005) 443.
[29] R. Hehl, G. Thiele, Z. Anorg. Allg. Chem. 626 (2000) 2167.
[30] D.L. Smith, V.I. Saunders, Acta Crystallogr. B 37 (1981) 1807.
[31] E.V.A. Premalal, G.R.R.A. Kumara, R.M.G. Rajapakse, M. Shimomura, K. Murakami, A. Konno, Chem. Commun. 46 (2010) 3360.
[32] X.T. Zhang, T. Taguchi, H.B. Wang, Q.B. Meng, O. Sato, A. Fujishima, Res. Chem. Intermed. 33 (2007) 5.
[33] G.R.A. Kumara, S. Kaneko, M. Okuya, K. Tennakone, Langmuir 18 (2002) 10493.
[34] I. Mora-Seró, S. Giménez, F. Fabregat-Santiago, E. Azaceta, R. Tena-Zaera, J. Bisquert, Phys. Chem. Chem. Phys. 13 (2011) 7162.
[35] F. Fabregat-Santiago, J. Bisquert, L. Cevey, P. Chen, M. Wang, S.M. Zakeeruddin, M. Grätzel, J. Am. Chem. Soc. 131 (2009) 558.
[36] E.V.A. Premalal, R.M.G. Rajapakse, A. Konno, Electrochim. Acta 56 (2011) 9180.
[37] F. Fabregat-Santiago, J. Bisquert, G. Garcia-Belmonte, G. Boschloo, A. Hagfeldt, Sol. Energy Mater. Sol. Cells 87 (2005) 117.
[38] N. Golego, S.A. Studenikin, M. Cocivera, Surface Canada 1997 May 21–24, Université de Sherbrooke, Sherbrooke, Que., Canada, 1997.
[39] A. Nasu, S. Yamaguchi, T. Sekine, Anal. Sci. 13 (1997) 903.